Oil Shale, 2015, Vol. 32, No. 2, pp. 109–123
doi: 10.3176/oil.2015.2.02
ISSN 0208-189X

Sr AND Nd ISOTOPIC SYSTEMATICS OF MID-CRETACEOUS ORGANIC-RICH ROCKS (OIL SHALES) FROM THE QIANGTANG BASIN: IMPLICATIONS FOR SOURCE REGIONS AND SEDIMENTARY PALEOENVIRONMENT

XIUGEN FU[(a,b)*], JIAN WANG[(a,b)], FUWEN TAN[(a,b)], XINGLEI FENG[(a)], WENBIN CHEN[(a)], CHUNYAN SONG[(a,b)], SHENGQIANG ZENG[(a)]

[(a)] Chengdu Institute of Geology and Mineral Resources, Chengdu 610081, China
[(b)] Key Laboratory for Sedimentary Basin and Oil and Gas Resources, Ministry of Land and Resources, Chengdu 610081, China

Abstract. *The Mid-Cretaceous oil shale from the Qiangtang Basin represents the potentially largest marine oil shale resource in China. 23 samples, including oil shale and marl, were collected from the Basin's Shengli River area to determine Sr and Nd isotope compositions, discuss sedimentary sources and paleoenvironmental changes. The Nd isotopic compositions of the Shengli River oil shale are similar to those of the Nadi Kangri Formation volcanic rocks and the underlying Suowa Formation limestone, indicating the Nadi Kangri Formation volcanic rocks and the Suowa Formation limestone origins of oil shale. The T_{Dm} ages of oil shale may be considered as the mean age of the upper continental crust in the Qiangtang Basin. Therefore, just like other fine-grained continental sediments, oil shale comprises sampled source rocks that were particularly well mixed through multiple stages of sedimentary recycling. The oil shale samples from the Shengli River area have higher $^{87}Sr/^{86}Sr$ ratios than the contemporary seawater. The high $^{87}Sr/^{86}Sr$ ratio reflects the Sr isotope composition of their original precipitation fluids. Marl samples from this area exhibit slightly higher $^{87}Sr/^{86}Sr$ ratios (mean = 0.7084) than oil shale samples (mean = 0.7076), and show a dramatic Sr isotopic shift near the boundary between the oil shale seams and marl beds. This shift is closely correlated with a rapid change in Nd isotopic compositions, indicating paleoenvironmental changes across the oil shale-marl boundary.*

Keywords: *Cretaceous marine oil shale, Sr-Nd isotope, source regions, sedimentary paleoenvironment, Qiangtang Basin.*

[*] Corresponding author: email *fuxiugen@126.com*

1. Introduction

Significant changes in the Mid-Cretaceous time are one of the most important global geological events [1, 2]. During that period, extensive oil shale deposits were formed in the Qiangtang Basin [3, 4]. These deposits represent the potentially largest marine oil shale resource in China [4]. The oil shale deposition in the Qiangtang Basin signifies also the latest accumulation of marine sediments in it.

In the last decades, quite a number of studies have been carried out to investigate the concentration and distribution of major and trace elements, especially rare earth elements (REEs), in organic-rich rocks (e.g., oil shale) [5–7], because these tracers can provide important information on provenance, sedimentary paleoenvironment, and sediment recycling [6, 7]. Compared to chemical composition, the isotopic characteristics of oil shale are of relatively less concern. Strontium and neodymium isotopes have been successfully applied to characterize sediment provenance and reconstruct spatial and temporal variations of sediment supply to basins [8] because Sr-Nd isotope ratios are thought to bear a fingerprint of source rocks. The Sr and Nd isotope compositions can also provide unique information about paleoenvironmental changes [9–11].

In the present study, Sr and Nd isotopic data for the Cretaceous oil shale from the Qiangtang Basin, northern Tibet, China, have been analyzed. The aim of this paper is: (1) to discuss sediment sources of organic-rich rocks; and (2) to reconstruct paleoenvironmental changes, as recorded by the respective change in the oil shale section.

2. Geological setting

The Qiangtang block, marked by the Hoh Xil-Jinsha River suture zone (HJS) to the north and the Bangong Lake-Nujiang River suture zone (BNS) to the south, respectively (Fig. 1a), consists of the North Qiangtang depression, the Central uplift and the South Qiangtang depression (Fig. 1b) [12]. During the Cretaceous, the Bangong Ocean closed by the northward subduction beneath the Qiangtang terrane [12], resulting in a large-scale regression in the Qiangtang Basin [13]. During this interval, the South Qiangtang depression was uplifted entirely, while the North Qiangtang depression was still a depositional area. Sedimentary rocks of this stage are mainly made up of sandstone, shale, marl, micritic limestone, oolitic limestone, mudstone and oil shale.

The Shengli River-Changshe Mountain oil shale zone is located in the southern part of the North Qiangtang depression (Fig. 1b), comprising the Shengli River oil shale and the Changshe Mountain oil shale. This zone is exposed for a distance of more than 50 km in an east-west direction and 30 km in a north-south direction (Fig. 1c). The proven reserves of the

Shengli River-Changshe Mountain oil shale have been estimated to exceed 1.0×10^9 tonnes [4], being potentially the largest marine oil shale resource in China.

A gradual lateral variation in oil shale seam is an important feature of the Shengli River-Changshe Mountain oil shale [4]. The oil shale sequence

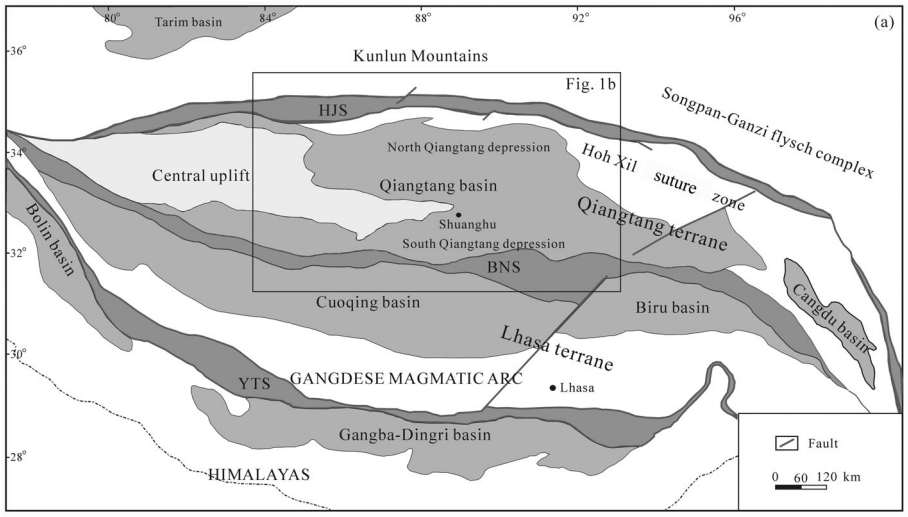

Fig. 1a. Map of the Tibetan Plateau showing major terranes (after [7]). HJS – Hoh Xil-Jinsha River suture; BNS – Bangong Lake-Nujiang River suture; YTS – Yarlung Tsangpo suture; HMLY – Himalayas.

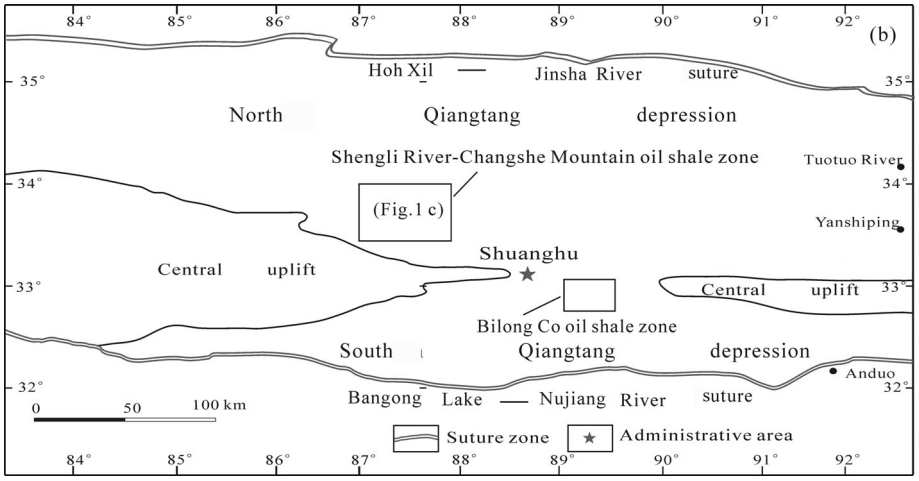

Fig. 1b. Generalized map showing the location of the study area (modified from [14]).

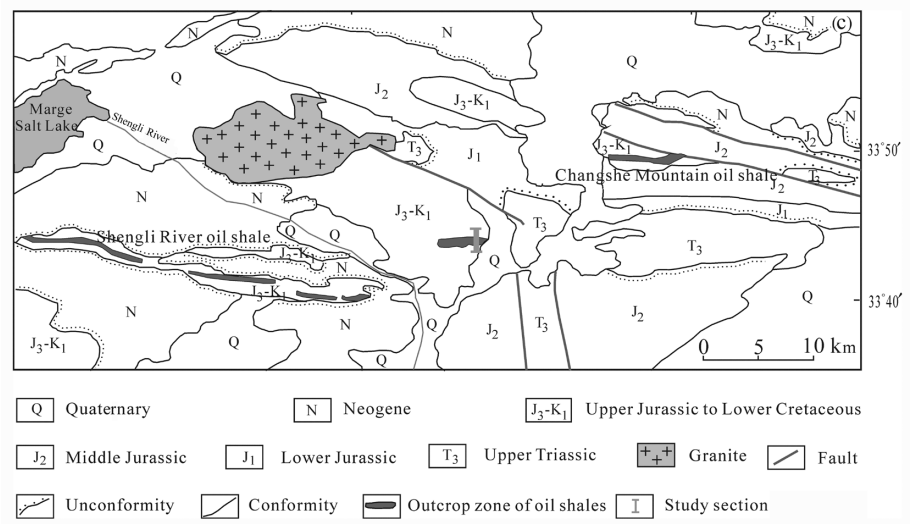

Fig. 1c. Simplified geological map of the Shengli River area showing the location of the oil shale section (after [14]).

consists of seven intervals in the middle part of the oil shale zone, with a thickness of 0.92 m to 2.21 m for individual intervals. However, only four oil shale seams can be identified in the western and eastern parts of the oil shale zone, where the thickness of individual seams is from 0.59 to 0.93 m [4]. The Re-Os isotope and biostratigraphic data suggest that the oil shale is Mid-Cretaceous (ca. 101 Ma) [3].

3. Sampling and analytical methods

The studied section is located in the Shengli River area, in the middle part of the Shengli River-Changshe Mountain oil shale zone (Fig. 1c). A total of 23 fresh unmetamorphosed samples were collected from this section, eighteen of them were taken from oil shale seams with a vertical sampling interval of 25 cm on average, and the other five samples were collected from marl beds. The oil shale samples show higher organic content (9.42–15.38%) compared to marl samples (0.63–2.32%) [14].

Fresh rock samples were powdered to 200 mesh in an agate mill. The ground samples were first baked at 700 °C to destroy organic materials, prior to Sr-Nd isotopic analysis. Sr isotopes were measured on a GV Isoprobe-T thermal ionization mass spectrometer (TIMS) at the Institute of Geology and Geophysics, Chinese Academy of Sciences. The analytical technique described by Ma et al. [15] was followed. $^{88}Sr/^{86}Sr = 0.1194$ was adopted to calibrate mass bias during measurements, and the NBS 987 Sr standard was repeatedly measured to monitor the quality of measurements, yielding

an average $^{87}Sr/^{86}Sr$ of 0.710265 ± 0.000009 (2σ; N = 24). Nd isotopic measurements were carried out on a MicroMass Isoprobe multi-collector inductively coupled plasma mass spectrometer (MC-ICP-MS) at the Guangzhou Institute of Geochemistry, Chinese Academy of Sciences. The analytical procedures have been described by Liang et al. [16]. Fractionation of the measured $^{143}Nd/^{144}Nd$ was normalized using $^{146}Nd/^{144}Nd = 0.7219$. A standard Nd solution, Shin-Etsu JNDi-1, was repeatedly measured together with the samples, and yielded a mean $^{143}Nd/^{144}Nd$ value of 0.512118 ± 0.000009 (2σ; N = 20). The accuracy of measurements of isotope concentrations and Sm/Nd ratios was higher than 2%. The mineral phases were determined by optical microscopic observation.

4. Results

Isotopic data for oil shale and marl samples from the Shengli River area are graphically presented as initial $^{87}Sr/^{86}Sr$ vs. initial ε_{Nd} in Figure 2 and tabulated in Table 1. Sr and Nd isotopic ratios are age-corrected to the 101 Ma age based on the oil shale Re-Os age and spore and pollen assemblages [3].

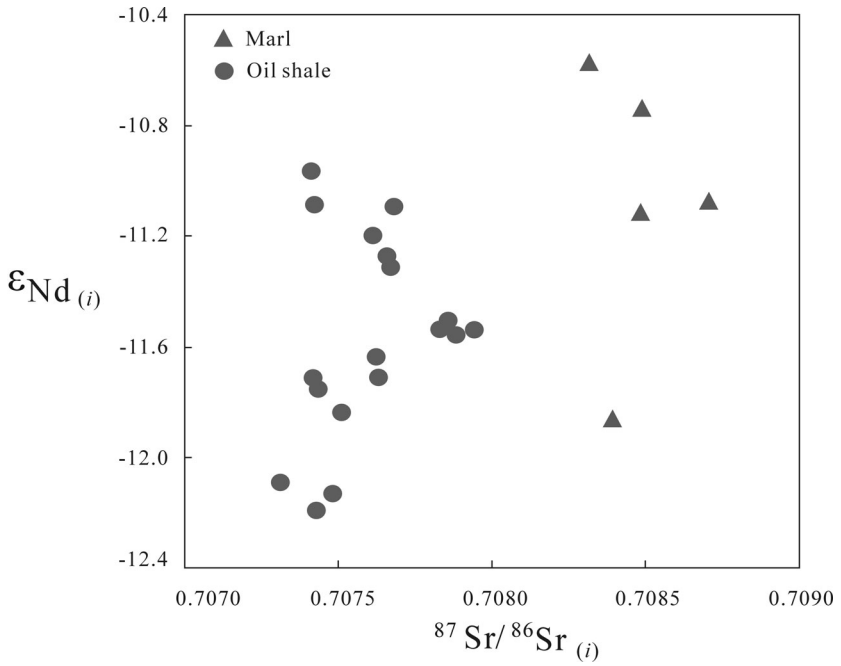

Fig. 2. $^{87}Sr/^{86}Sr_{(i)}$ vs. $\varepsilon_{Nd(i)}$ values for the samples studied, exhibiting a strong difference between oil shale and marl samples.

Table 1. Sr and Nd isotope data and selected major and trace elements of oil shale and marl samples from the Shengli River area (element content including SiO_2, Al_2O_3, CaO, MnO, Rb, Sr, Sm, Nd, Zr and ∑REE values after [14].)

Sample	Lithology	Rb, ppm	Sr, ppm	$^{87}Rb/^{86}Sr$	$^{87}Sr/^{86}Sr$	2σ	$(^{87}Sr/^{86}Sr)_i$	Sm, ppm	Nd, ppm	$^{147}Sm/^{144}Nd$	$^{143}Nd/^{144}Nd$	2σ	$(^{143}Nd/^{144}Nd)_i$	$\varepsilon_{Nd}(0)$	$\varepsilon_{Nd}(i)$	T_{Dm}, Ga	SiO_2, %	CaO, %	MnO, %	Al_2O_3, %	Zr, ppm	∑REE, ppm
SL-1	Marl	69.21	446.6	0.4509	0.708966	0.000016	0.70832	2.22	11.72	0.1145	0.512042	0.000006	0.511966	–11.6	–10.6	1.70	20.16	36.93	0.021	5.54	63.11	66.34
SL-2	Marl	77.41	428.5	0.5256	0.709234	0.000018	0.70848	2.19	11.77	0.1126	0.512013	0.000008	0.511939	–12.2	–11.1	1.71	13.49	21.54	0.021	3.83	67.91	67.67
SL-3	Marl	75.67	436.0	0.5049	0.709213	0.000020	0.70849	2.18	12.08	0.1091	0.512030	0.000006	0.511958	–11.9	–10.7	1.63	14.89	24.46	0.023	4.29	65.95	68.31
SL-4	Marl	74.07	407.2	0.5292	0.709466	0.000018	0.70871	2.25	12.06	0.1126	0.512015	0.000006	0.511941	–12.2	–11.1	1.71	20.23	34.06	0.025	5.67	62.81	67.77
SL-5	Marl	70.28	432.7	0.3937	0.708959	0.000017	0.70839	2.24	11.78	0.1141	0.511975	0.000005	0.511900	–12.9	–11.9	1.80	19.96	32.69	0.026	5.33	55.57	63.86
SL-6	Oil shale	50.39	557.1	0.2631	0.708316	0.000014	0.70794	1.96	9.76	0.1214	0.511997	0.000006	0.511917	–12.5	–11.5	1.90	15.45	37.15	0.032	3.70	47.65	55.20
SL-7	Oil shale	39.25	561.1	0.2035	0.707950	0.000014	0.70766	1.77	8.88	0.1205	0.512010	0.000006	0.511930	–12.3	–11.3	1.86	13.30	38.32	0.037	3.13	42.99	49.71
SL-8	Oil shale	49.08	605.0	0.236	0.708172	0.000011	0.70783	1.95	9.85	0.1198	0.511996	0.000006	0.511917	–12.5	–11.5	1.87	15.78	36.23	0.039	3.73	47.01	55.01
SL-9	Oil shale	50.22	2365.2	0.0618	0.707518	0.000018	0.70743	1.84	9.56	0.1161	0.511960	0.000006	0.511883	–13.2	–12.2	1.86	16.58	36.62	0.052	4.03	44.56	54.70
SL-10	Oil shale	53.75	1327.0	0.1178	0.707650	0.000013	0.70748	1.97	10.09	0.1177	0.511964	0.000006	0.511886	–13.1	–12.1	1.88	18.32	35.92	0.057	4.33	49.34	55.18
SL-11	Oil shale	49.29	966.2	0.1484	0.707723	0.000014	0.70751	1.94	9.74	0.1206	0.511981	0.000005	0.511901	–12.8	–11.8	1.91	15.96	37.52	0.053	3.77	48.29	55.25
SL-12	Oil shale	59.04	627.1	0.2739	0.708250	0.000018	0.70786	2.23	11.18	0.1203	0.511998	0.000006	0.511919	–12.5	–11.5	1.88	17.54	35.43	0.060	4.26	48.94	53.98
SL-13	Oil shale	52.66	695.7	0.2202	0.707982	0.000018	0.70767	2.08	10.39	0.1212	0.512009	0.000007	0.511929	–12.3	–11.3	1.88	16.38	36.93	0.052	3.95	47.39	56.50
SL-14	Oil shale	42.11	1010.5	0.1212	0.707583	0.000016	0.70741	1.72	8.36	0.124	0.512028	0.000007	0.511946	–11.9	–11.0	1.91	13.30	39.25	0.043	3.53	37.02	47.77
SL-15	Oil shale	39.86	1029.8	0.1126	0.707585	0.000013	0.70742	1.68	8.15	0.1244	0.512022	0.000005	0.511940	–12.0	–11.1	1.92	12.84	40.43	0.039	3.31	36.61	46.91
SL-16	Oil shale	44.3	1095.2	0.1177	0.707606	0.000014	0.70744	1.74	8.76	0.1201	0.511985	0.000007	0.511906	–12.7	–11.8	1.90	14.13	40.43	0.034	3.46	40.19	50.33
SL-17	Oil shale	37.99	964.2	0.1146	0.707585	0.000013	0.70742	1.7	8.23	0.1246	0.511990	0.000007	0.511908	–12.6	–11.7	1.98	12.94	41.99	0.031	2.95	34.05	45.43
SL-18	Oil shale	40.27	1338.6	0.0875	0.707438	0.000016	0.70731	1.48	7.3	0.1223	0.511969	0.000009	0.511888	–13.1	–12.1	1.97	12.88	39.44	0.035	3.12	37.02	48.94
SL-19	Oil shale	49.96	1229.6	0.01182	0.707701	0.000013	0.70768	1.96	9.74	0.1218	0.512020	0.000005	0.511940	–12.1	–11.1	1.87	16.09	39.25	0.029	4.07	46.28	52.90
SL-20	Oil shale	58.81	879.9	0.1944	0.707890	0.000013	0.70761	2.22	11.12	0.1207	0.512014	0.000006	0.511934	–12.2	–11.2	1.86	18.52	36.42	0.035	4.63	42.01	52.93
SL-21	Oil shale	58.83	805.9	0.2124	0.707929	0.000014	0.70762	2.16	10.7	0.1221	0.511992	0.000007	0.511911	–12.6	–11.6	1.93	19.47	35.89	0.034	4.74	41.45	51.30
SL-22	Oil shale	67.2	772.1	0.2532	0.708245	0.000013	0.70788	2.37	11.8	0.1215	0.511996	0.000006	0.511916	–12.5	–11.6	1.91	20.71	34.67	0.035	5.00	45.8	52.89
SL-23	Oil shale	52.08	748.0	0.2025	0.707919	0.000011	0.70763	2.01	9.92	0.1227	0.511989	0.000007	0.511908	–12.7	–11.7	1.94	18.37	37.04	0.031	4.59	45.88	52.36

4.1. Strontium isotopes

Strontium concentrations of oil shale samples are over 557.1 ppm, with a maximum of 2365.2 ppm and an average of 976.6 ppm (Table 1). In contrast, marl samples exhibit a lower Sr concentration ranging between 407.2 and 482.7 ppm, with an average of 430.2 ppm. All samples exhibit low Rb/Sr ratios ranging from 0.02 to 0.18. The $^{87}Sr/^{86}Sr$ ratios of samples cluster into discrete groups with minimal overlap: 0.70731–0.70794 for the oil shale group, and 0.70832–0.70871 for the marl group (Fig. 2). Generally, the Sr isotopic ratios show an abrupt increase upwards from the oil shale seams to marl beds.

4.2. Neodymium isotopes

The measured $^{147}Sm/^{144}Nd$ values for oil shale samples from the Shengli River area vary from 0.116 to 0.125 (Table 1), marl samples generally having slightly lower $^{147}Sm/^{144}Nd$ values (0.109–0.115). The oil shale samples have overlapping $\varepsilon_{Nd}(0)$ values ranging from –13.2 to –11.9, while those of marl samples vary between –12.9 and –11.6. Overall, the present-day Nd isotopic compositions show an increase towards comparatively more radiogenic values from the oil shale seams to marl beds.

4.3. Minerals in oil shale seams

Microscopic observation reveals that the mineral component of oil shale samples accounts normally for more than 50% by volume, varying between 51.3% and 72.5%. It mainly consists of carbonates (22.5–44.3%), quartz (7.0–16.3%), clay minerals (16.2–36.5%) and pyrite (0.4–3.3%). Clay minerals are common in the oil shale samples. They occur in thin-layered and massive forms [14]. The calcite content in the Shengli River oil shale samples is high, calcite existing mainly as disseminated fine particles [14]. Abundant fossil shells were also found in the samples. The shell material was found to be nearly pure calcite. The negative relationship (r = –0.24) between Ca and Al contents indicates that calcite is not of detrital origin.

5. Discussion

5.1. Occurrence of Rb, Sr, Sm and Nd

The mode of occurrence of elements in oil shale can be inferred from its association with particular minerals or major elements [7] based on Pearson's coefficients of correlation between elements. Coarse-grained detrital minerals are rare in the Shengli River oil shale; the absorption of fine-grained minerals and/or organic matter may be the main mode of occurrence of Rb, Sr, Sm and Nd. Note that Rb, Sm and Nd concentrations are positively correlated with ash yield [14], which shows that detrital minerals in oil shale seams are the main carriers of these elements. The significantly

positive correlations between Si concentration and Rb (r = 0.96), Sm (r = 0.90) and Nd (r = 0.92) contents, and Al concentration and Rb (r = 0.94), Sm (r = 0.88) and Nd (r = 0.88) contents indicate that Rb, Sm and Nd are mainly present in clay minerals.

Strontium exhibits a negligible correlation with ash yield [14], suggesting that this element is present probably in more than one form.

5.2. Neodymium isotope composition and source of oil shale

Neodymium isotopes can provide important information about the provenance of clastic sediments in marine environments [17]. The present-day $\varepsilon_{Nd}(0)$ values and $^{147}Sm/^{144}Nd$ ratios in oil shale and marl samples are relatively uniform, with a small variation between –13.2 and –11.6, and from 0.1091 to 0.1246, respectively, and the Sm-Nd model ages (or crustal residence ages) are restricted to a range of 1.63–1.98 Ga (Table 1). The depositional age of the Shengli River oil shale is about 101 Ma [3]. The obtained data suggest the detrital material origin. However, the Shengli River oil shale was formed in the Early Cretaceous. During that interval, large-scale regressions could have taken place in the Qiangtang Basin region. The deposition center was located in the northwestern part of the North Qiangtang depression, showing an asymmetric shape, i.e. deep in the west and shallow in the east. The potential sources (or sediment supply areas) for the sediments are located in the southern part (the Central uplift), the northern part (the Hoh Xil-Jinsha River suture zone), and the eastern part of the North Qiangtang depression, where the Nadi Kangri Formation (Late Triassic) volcanic rocks and the Suowa Formation (the underlying strata of oil shale) limestone are widely spread [12]. Additionally, the gravel components of the Xueshan Formation strata (contemporary strata of the Shengli River oil shale) mainly consist of the Nadi Kangri Formation and Suowa Formation gravels [12]. These data rule out the sediments as major source rocks for the oil shale in the Shengli River area. The $^{147}Sm/^{144}Nd$ values in oil shale samples reported here are similar to those of the Nadi Kangri Formation volcanic rocks (average 0.1267) (Table 2), and of the underlying Suowa Formation limestone (average 0.1215) (Table 2), indicating the Nadi Kangri Formation volcanic rocks and the Suowa Formation limestone origins of oil shale. Moreover, the model ages of the Shengli River oil shale are also similar to those of the Nadi Kangri Formation volcanic rocks (ca 1.7–1.9 Ga) (Table 2) and the Suowa Formation limestone (ca 1.8–1.9 Ga) (Table 2), which further supports the above observations. Therefore, just like other fine-grained continental sediments, oil shale comprises sampled source rocks that were particularly well mixed through multiple stages of sedimentary recycling. The T_{Dm} ages of oil shale may be considered as the mean age of the upper continental crust in the Qiangtang Basin.

Table 2. Sr and Nd isotope data of oil shale from the Shengli River area (SL) compared to those of Nadi Kangri Formation volcanic rocks (ND) and the underlying Suowa Formation limestone (SW) in the Qiangtang Basin (ND data are based on 25 samples, and SW data are based on 22 samples.)

Sample	Sr, ppm	$(^{87}Sr/^{86}Sr)_i$	$^{147}Sm/^{144}Nd$	T_{Dm}, Ga
ND	average 122.4	average 0.7125	average 0.1267	ca 1.7–1.9
SW	average 564.8	average 0.7073	average 0.1215	ca 1.8–1.9
SL	average 859.97	average 0.7078	average 0.1193	1.63–1.98

5.3. Strontium isotope composition and source of oil shale

In comparison with Nd isotopic compositions, $^{87}Sr/^{86}Sr$ ratios show a variation from 0.7074 to 0.7095. The isotope ratios of Sr are not significantly altered by the processes of weathering, transportation and deposition. Thus, during deposition the Shengli River oil shale should have recorded the isotope compositions of Sr in the latest Early Cretaceous seawater and/or sediment sources. The data of our study reveal that all the oil shale samples have higher $^{87}Sr/^{86}Sr$ ratios than the contemporary seawater. There are two possible explanations for this observation: (1) the Shengli River oil shale was diagenetically altered in association with radiogenic Sr addition after their precipitation, or (2) the precipitation fluid had high $^{87}Sr/^{86}Sr$ ratios. The Shengli River oil shale samples exhibit high Sr concentrations (482.7–2365.2 ppm), indicating that the siliciclastic materials did not contribute or contributed only a little to the strontium budget of oil shale during the diagenetic alteration. In addition, the oil shale samples from the Shengli River area are characterized by a low Mn concentration and a very low Mn/Sr ratio (0.21–0.96). This further indicates that the Shengli River oil shale was not significantly altered by diagenesis. Consequently, the high $^{87}Sr/^{86}Sr$ ratios for the oil shale samples from this area reflect the strontium isotope composition of their original precipitation fluids. In the present study, high $^{87}Sr/^{86}Sr$ ratios indicate a significant input of radiogenic ^{87}Sr to the system during deposition. The high $^{87}Sr/^{86}Sr$ ratio is indicative of the radiogenic strontium flux and its $^{87}Sr/^{86}Sr$ ratio was derived from tectonoclimatic processes such as the exposure and chemical weathering of ancient crystalline rocks with a high $^{87}Sr/^{86}Sr$ ratio. The exposed Nadi Kangri Formation felsic rocks contain on average 122.4 ppm of Sr and their $^{87}Sr/^{86}Sr$ ratio is 0.7125 (Table 2), while the Suowa Formation limestone exhibits a relatively low $^{87}Sr/^{86}Sr$ ratio (average 0.7073) and a high Sr content (average 564.8 ppm) (Table 2). Thus, the radiogenic strontium responsible for high $^{87}Sr/^{86}Sr$ ratios in oil shale samples probably originated from the Nadi Kangri felsic rocks. The positive correlations between $^{87}Sr/^{86}Sr$ ratio and SiO_2 (statistically significant at a strict significance level of 0.001; linear correlation coefficient $r = 0.51$) and Al_2O_3 ($r = 0.47$) contents further indicate that weathering clay minerals with more radiogenic Sr and lower Sr content should have had an important role in the detrital input to oil shale. The coefficient of correlation between

$^{87}Sr/^{86}Sr$ ratio and Al_2O_3 content is low, suggesting that radiogenic strontium has another source besides clay minerals. In the $^{87}Sr/^{86}Sr$ vs. 1/Sr diagram (Fig. 3), the linear trend for oil shale samples suggests a two-component mixing between the carbonate (low $^{87}Sr/^{86}Sr$, high Sr content) and silicate (high $^{87}Sr/^{86}Sr$, low Sr content) components.

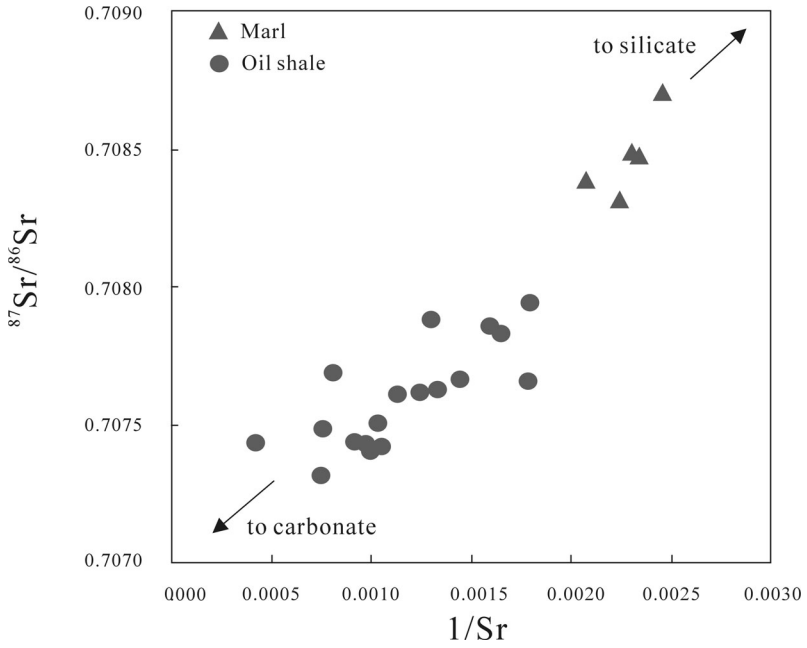

Fig. 3. $^{87}Sr/^{86}Sr$ vs. 1/Sr diagram for oil shale and marl samples from the Shengli River area, showing the two-component mixing.

5.4. Implications for sedimentary environment

Marl samples from the Shengli River area exhibit slightly higher $^{87}Sr/^{86}Sr$ ratios (mean = 0.7084) than oil shale samples (mean = 0.7076). At site SL-6, the $^{87}Sr/^{86}Sr$ ratio of oil shale is 0.70794, whereas that of marl is 0.70839 at site SL-5, exhibiting a dramatic Sr isotopic shift near the boundary between the oil shale seams and marl beds. The marl and oil shale samples both show high Sr concentrations (557.1–2365.2 ppm and 407.2–482.7 ppm, respectively), and low Mn/Sr ratios (0.21–0.96 and 0.47–0.61, respectively), excluding diagenetic alteration as an explanation for the increase in $^{87}Sr/^{86}Sr$ ratio from the oil shale seams to marl beds. Two other possible explanations for the increase in $^{87}Sr/^{86}Sr$ ratio at site SL-5 are: (1) change in the oceanic circulation pattern, or (2) local or regional change in the Sr continental supply. However, two observations argue against the change in the oceanic circulation as an explanation for the increase of $^{87}Sr/^{86}Sr$ ratio upwards from the oil shale seams to marl beds. First, Sr has a very long oceanic residence

time, about 2.4 myr [18], whereas there is a rapid isotopic shift from the oil shale seams to marl beds in the Shengli River area. Second, if the increase in $^{87}Sr/^{86}Sr$ ratio at site SL-5 was the result of change in the oceanic circulation, the strontium isotopic increase was expected to occur in the seawater during the deposition of oil shale and marl. However, it was actually a decrease in seawater $^{87}Sr/^{86}Sr$ values during the Cenomanian period [19]. Consequently, the increase in $^{87}Sr/^{86}Sr$ ratio from the oil shale seams to marl beds (Table 1) indicates an increased input of siliciclastics, possibly related to large-scale regressions that took place in the Qiangtang Basin region. Our observation is also supported by Zhao et al. [20], who quite recently reported that the enhanced continental weathering would increase the seawater $^{87}Sr/^{86}Sr$ ratios [20]. In addition, the weathering of Rb enriched minerals, such as micas and feldspars, will increase $^{87}Sr/^{86}Sr$ ratios in surface water [21]. The rapid increase in Rb content at site SL-5 (Fig. 4) in the Shengli River area further indicates a change in the $^{87}Sr/^{86}Sr$ values of regional continental inputs.

The oil shale seams (the lower units of the Shengli River Formation) are grey black in colour, well-laminated and with abundant fossils. Sedimentary structures such as horizontal bedding, ripple bedding and rhythmic bedding are well developed, indicating a lagoonal environment (semi-enclosed marginal marine environment). In contrast, the upper units of the Shengli River Formation are mainly composed of grey black marl intercalated with gypsum salt. Sedimentary structures such as lattice structure and finely-laminated bedding are well developed and indicate a hot and arid lagoon environment. The Shengli River Formation sequence, thus, records a shallowing-upward sequence and can be interpreted as an increased input of siliciclastics during deposition of marl and gypsum salt (the overlying strata of oil shale). Additionally, the Sr ratio increase at site SL-5 is closely correlated with the 29.0% and 35.7% increases respectively in Si and Al contents from the oil shale seams to marl beds (Fig. 4), which further supports the opinion that enhanced continental weathering could have played an important role in Sr ratio increase from the oil shale seams to marl beds.

The Shengli River oil shale and marl are also shown to differ in $^{147}Sm/^{144}Nd$ ratio, which is respectively 0.1161–0.1246 and 0.1091–0.1145 (Fig. 4). Nd model ages are younger for marl (T_{Dm} = 1.63–1.80 Ga) than for oil shale (1.86–1.98 Ga), and $\varepsilon_{Nd}(i)$ values also show slight differences between oil shale (–12.2 to –11.0) and marl (–11.9 to –10.6) (Fig. 4). Given the fine-grained nature of the sediments analyzed, the uniformity of chemical data within each series and the absence of heavy mineral accumulation or significant REE distribution, it is considered that Nd isotope data reflect the average sampling of their source rocks [22]. The Sm-Nd isotopic shift from the oil shale seams to marl beds should record a slightly various source region. As discussed above, large-scale regressions may have taken place in the Qiangtang Basin during the Early Cretaceous time. As a result, when the relative sea level was low, most parts of the Basin were uplifted into a land

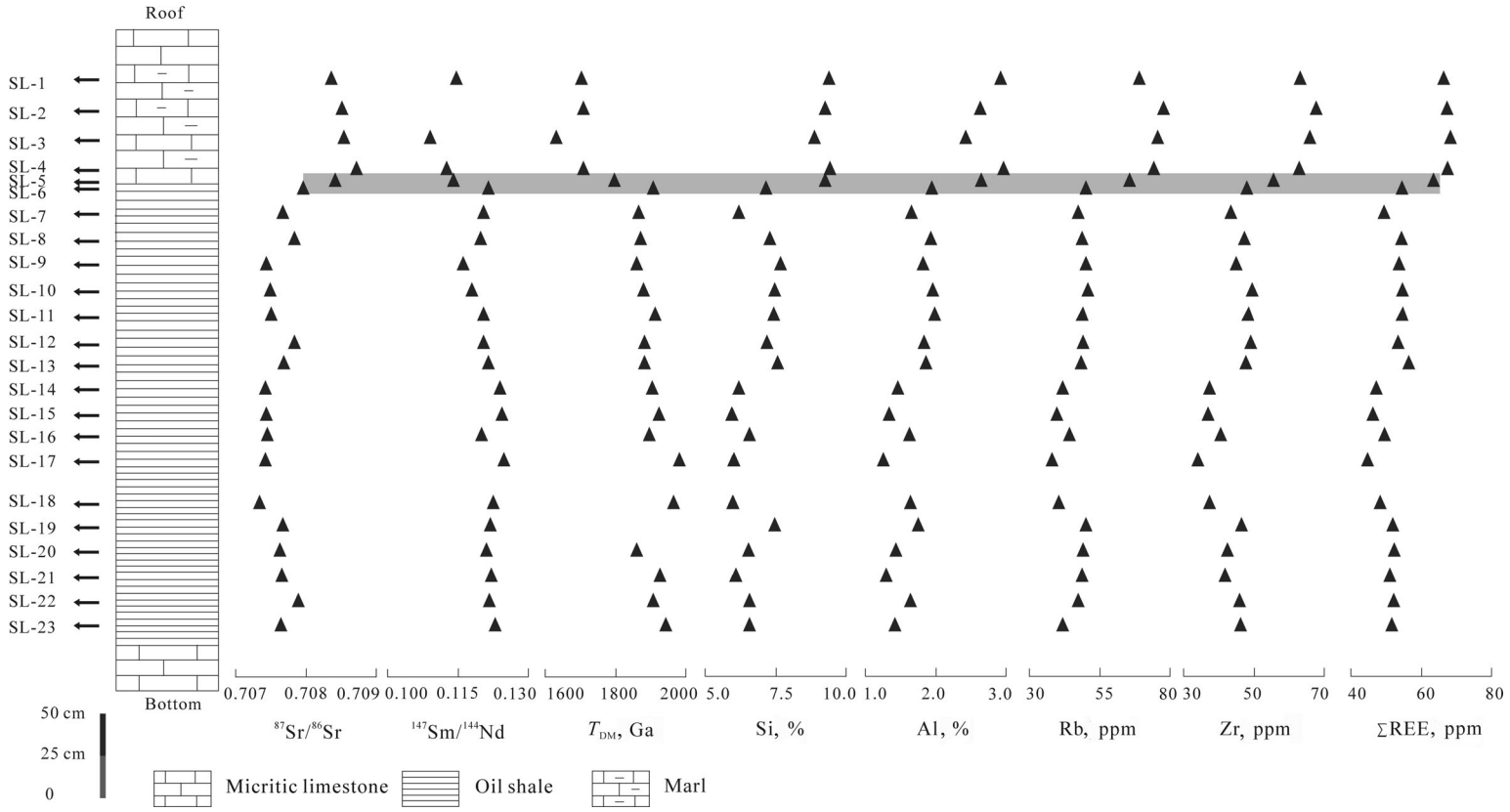

Fig. 4. Vertical variations of Sr-Nd isotopes, ∑REE and selected major and trace elements contents in the Shengli River area, indicating a dramatic shift at the boundary between the oil shale seams and marl beds (Si, Al, Zr and ∑REE values after [14]).

corresponding to an enhanced continental weathering. As discussed by Macleod et al. [23], if weathering inputs changed dramatically, the ε_{Nd} of seawater would shift without requiring any change in ocean processes. Additionally, a study of the Nadi Kangri volcanic rocks indicates that the lower part of the Nadi Kangri volcanic sequences exhibits a slightly higher $\varepsilon_{Nd}(i)$ than upper sequences [12]. These data further support the belief that enhanced continental weathering and large-scale regressions probably played an important role in Sm-Nd isotopic shift from the oil shale seams to marl beds.

Frimmel speculated that trace element distributions in carbonates can be useful monitors of their depositional palaeoenvironment [18]. Low Zr, Rb and total rare earth element (∑REE) contents reflect a distal depositional environment, while high Zr, Rb and ∑REE contents are probably related to a near-shore environment. In the Shengli River area, the oil shale seams exhibit relatively low Zr (average 43.5 ppm), Rb (average 46.5 ppm) and ∑REE (average 52.1 ppm) contents (Fig. 4) [14], which is indicative of a semi-enclosed marginal marine environment [4]. In contrast, the marl beds in this area show higher Zr (average 63.1 ppm), Rb (average 72.3 ppm) and ∑REE (average 66.8 ppm) contents (Fig. 4), reflecting a larger continental detrital component in a more near-shore environment (evaporation lagoon).

6. Conclusions

(1) The Nd isotopic compositions in oil shale samples from the Shengli River area are similar to those of the Nadi Kangri Formation volcanic rocks and the underlying Suowa Formation limestone, indicating the Nadi Kangri Formation volcanic rocks and the Suowa Formation limestone origins of the oil shale material. The T_{Dm} ages of oil shale may be considered as the mean age of the upper continental crust in the Qiangtang Basin. Therefore, just like other fine-grained continental sediments, oil shale comprises sampled source rocks that were particularly well mixed through multiple stages of sedimentary recycling.

(2) Oil shale samples from the Shengli River area have higher $^{87}Sr/^{86}Sr$ ratios than the contemporary seawater. The high $^{87}Sr/^{86}Sr$ ratio reflects the strontium isotope composition of their original precipitation fluids.

(3) The boundary between the oil shale seams and marl beds is characterized by abrupt changes in Sr isotopic composition in the marl beds having more radiogenic Sr isotopic compositions compared to the oil shale seams. This indicates changes in provenance with sediments in the marl beds being derived from more near-shore sources compared to the oil shale seams. This is also supported by changes in Nd isotopic compositions across this boundary. The strikingly different trace element patterns of marl beds compared to the underlying oil shale seams also to

speak in support of paleoenvironmental changes across the oil shale to marl boundary.

Acknowledgements

This work was supported by the National Natural Science Foundation of China (Nos. 41172098, 40972087, 40702020), the Sichuan Youth Science & Technology Foundation (No. 09ZQ026-006), and the National Oil and Gas Special Project (No.XQ-2009-01).

REFERENCES

1. Wan, X. Q., Wei, M. R., Li, G. B. $\delta^{13}C$ values from the Cenomanian-Turonian passage beds of southern Tibet. *J. Asian Earth Sci.*, 2003, **21**(8), 861–866.
2. Hu, X. M., Wagreich, M., Yilmaz, I. O. Marine rapid environmental/climatic change in the Cretaceous greenhouse world. *Cretaceous Res.*, 2012, **38**, 1–6.
3. Fu, X. G., Wang, J., Qu, W. J., Duan, T. Z., Du, A. D., Wang, Z. J., Liu, H. Re-Os (ICP-MS) dating of marine oil shale in the Qiangtang Basin, northern Tibet, China. *Oil Shale*, 2008, **25**(1), 47–55.
4. Fu, X. G., Wang, J., Tan, F. W., Zeng, Y. H. Sedimentological investigations of the Shengli River-Changshe Mountain oil shale (China): relationships with oil shale formation. *Oil Shale*, 2009, **26**(3), 373–381.
5. Sonibare, O. O., Jacob, D. E., Ward, C. R., Foley, S. F. Mineral and trace element composition of the Lokpanta oil shales in the Lower Benue Trough, Nigeria. *Fuel*, 2011, **90**(9), 2843–2849.
6. Stein, M., Westermann, S., Adatte, T., Matera, V., Fleitmann, D., Spangenberg, J. E., Föllmi, K. B. Late Barremian-Early Aptian palaeoenvironmental change: The Cassis-La Bédoule section, southeast France. *Cretaceous Res.*, 2012, **37**, 209–222.
7. Fu, X. G., Wang, J., Zeng, Y. H., Tan, F. W., Feng, X. L. Concentration and mode of occurrence of trace elements in marine oil shale from the Bilong Co area, Northern Tibet, China. *Int. J. Coal Geol.*, 2011, **85**(1), 112–122.
8. Krom, M. D., Michard, A., Cliff, R. A., Strohle, K. Sources of sediment to the Ionian Sea and western Levantine basin of the Eastern Mediterranean during S-1 sapropel times. *Mar. Geol.*, 1999, **160**(1–2), 45–61.
9. Weldeab, S., Siebel, W., Wehausen, R., Emeis, K.-C., Schmiedl, G., Hemleben, C. Late Pleistocene sedimentation in the Western Mediterranean Sea: implications for productivity changes and climatic conditions in the catchment areas. *Palaeogeogr. Palaeocl.*, 2003, **190**, 121–137.
10. Fu, X. G., Wang, J., Zeng, Y. H., Tan, F. W., Feng, X. L. Source regions and the sedimentary paleoenvironment of marine oil shale from the Bilong Co area, northern Tibet, China: an Sr-Nd isotopic study. *Oil Shale*, 2012, **29**(4), 306–321.
11. Baioumy, H. Rare earth elements and sulfur and strontium isotopes of Upper Cretaceous phosphorites in Egypt. *Cretaceous Res.,* 2011, **32**(3), 368–377.
12. Wang, J., Ding, J., Wang, C. S., Tan, F. W., Chen, M., Hu, P., Li, Y. L., Gao, R., Fang, H., Zhu, L. D., Li, Q. S., Zhang, M. H., Du, B. W., Fu, X. G.,

Li, Z. X., Wan, F. *Survey and Evaluation on Tibet Oil and Gas Resources*. Beijing: Geological Publishing House, Beijing, 2009, 11–223 (in Chinese).
13. Fu, X. G., Wang, J., Tan, F. W., Chen, M., Chen, W. B. The Late Triassic rift-related volcanic rocks from eastern Qiangtang, northern Tibet (China): Age and tectonic implications. *Gondwana Res.*, 2010, **17**(1), 135–144.
14. Fu, X. G., Wang, J., Zeng, Y. H., Cheng, J., Tan, F. W. Origin and mode of occurrence of trace elements in marine oil shale from the Shengli River area, northern Tibet, China. *Oil Shale*, 2011, **28**(4), 487–506.
15. Ma, J. L., Wei, G. J., Xu, Y. G., Long, W. G. Variations of Sr-Nd-Hf isotopic systematics in basalt during intensive weathering. *Chem. Geol.*, 2010, **269**(3–4), 376–385.
16. Liang, X. R., Wei, G. J., Li, X. H., Liu, Y. Precise measurement of $^{143}Nd/^{144}Nd$ and Sm/Nd ratios using multiple-collectors inductively coupled plasma-mass spectrometry (MC-ICPMS). *Geochimica*, 2003, **32**, 91–96 (in Chinese with English abstract).
17. Farmer, G. L., Ball, T. T. Sources of Middle Proterozoic to Early Cambrian siliciclastic sedimentary rocks in the Great Basin: A Nd isotope study. *Bull. Geol. Soc. Am.*, 1997, **109**(9), 1193–1205.
18. Frimmel, H. E. Trace element distribution in Neoproterozoic carbonates as palaeoenvironmental indicator. *Chem. Geol.*, 2009, **258**(3–4), 338–353.
19. Baioumy, H. Rare earth elements and sulfur and strontium isotopes of upper Cretaceous phosphorites in Egypt. *Cretaceous Res.*, 2011, **32**(3), 368–377.
20. Zhao, Y. Y., Zheng, Y. F., Chen, F. K. Trace element and strontium isotope constraints on sedimentary environment of Ediacaran carbonates in southern Anhui, South China. *Chem. Geol.*, 2009, **265**(3–4), 345–362.
21. Lan, C. Y., Lee, C. S., Shen, J. J., Lu, C. Y., Mertzman, S. A., Wu, T. W. Nd-Sr isotopic composition and geochemistry of sediments from Taiwan and their implications. *Western Pacific Earth Sci.*, 2002, **2**(2), 205–222.
22. Ugidos, J. M., Valladares, M. I., Recio, C., Rogers, G., Fallick, A. E., Stephens, W. E. Provenance of Upper Precambrian-Lower Cambrian shales in the Central Iberian Zone, Spain: evidence from a chemical and isotopic study. *Chem. Geol.*, 1997, **136**(1–2), 55–70.
23. MacLeod, K. G., Martin, E. E., Blair, S. W. Nd isotopic excursion across Cretaceous ocean anoxic event 2 (Cenomanian-Turonian) in the tropical North Atlantic. *Geology*, 2008, **36**(10), 811–814.

Presented by A. Soesoo
Received February 19, 2014